The Journal of Experimental Biology 207, 4623-4631
Published by The Company of Biologists 2004
doi:10.1242/jeb.01333

Ion-motive ATPases and active, transbranchial NaCl uptake in the red freshwater crab, *Dilocarcinus pagei* (Decapoda, Trichodactylidae)

Dirk Weihrauch[1,*], John Campbell McNamara[2], David W. Towle[3] and Horst Onken[4]

[1]*Department of Animal Physiology, University of Osnabrueck, 49076 Osnabrueck, Germany*, [2]*Departamento de Biologia, Faculdade de Filosofia, Ciências e Letras de Ribeirão Preto, Universidade de São Paulo, Avenida Bandeirantes 3900, Ribeirão Preto 14040-901, São Paulo, Brasil*, [3]*Mount Desert Island Biological Laboratory, Salsbury Cove, ME 04672, USA* and [4]*School of Biological Sciences, Washington State University, Pullman, WA 99164-4236, USA*

*Author for correspondence (e-mail: weihrauch@biologie.uni-osnabrueck.de)

Accepted 5 October 2004

Summary

The present investigation examined the microanatomy and mRNA expression and activity of ion-motive ATPases, in anterior and posterior gills of a South American, true freshwater crab, *Dilocarcinus pagei*. Like diadromous crabs, the anterior gills of this hololimnetic trichodactylid exhibit a highly attenuated (2–5 μm), symmetrical epithelium on both lamellar surfaces. In sharp contrast, the posterior gill lamellar epithelia are markedly asymmetrical. Their proximal side consists of thick (18–20 μm) cells, displaying features typical of a transporting epithelium, while the distal epithelium is thin (3–10 μm) and formed entirely by apical pillar cell flanges. Both anterior and posterior gills express Na^+/K^+- and V-ATPases. Phylogenetic analysis of partial cDNA sequences for the Na^+/K^+-ATPase α-subunit and V-ATPase B-subunit among various crab species confirmed the previous classification and grouping of *D. pagei* based on morphological criteria. Semi-quantitative RT-PCR clearly showed that mRNA for both ion pump subunits is more intensely expressed in posterior gills. Na^+/K^+-ATPase activity in the posterior gills was nearly fourfold that of anterior gills, while V-ATPase and F-ATPase activities did not differ. A negative short-circuit current (I_{sc}) was measured using the distal side of split, posterior gill lamellae, mounted in a modified Ussing chamber and perfused symmetrically with identical hemolymph-like salines. Although hemolymph-side ouabain did not affect this current, concanamycin significantly reduced I_{sc} without altering preparation conductance, suggesting V-ATPase-driven Cl^- absorption on the distal side of the posterior gill lamellae, as known to occur in diadromous crabs adapted to freshwater. These findings suggest that active Na^+ uptake predominates across the thick proximal epithelium, and Cl^- uptake across the thin, distal epithelium of the posterior gill lamellae.

Key words: osmoregulation, crab, *Dilocarcinus pagei*, gill epithelia, phylogenetic analysis, NaCl uptake, Na^+/K^+-ATPase, V-type H^+-ATPase, transepithelial voltage, short-circuit current, ouabain, concanamycin.

Introduction

Freshwater crustaceans, fish and amphibians are continuously challenged to maintain the ionic concentrations of their body fluids within strict physiological limits, while exposed to an extremely dilute medium containing less than 0.2 mmol l^{-1} NaCl. The epithelia of hyperosmoregulating crabs exhibit low permeabilities to ions and water, minimizing passive salt loss and osmotic water entry across the body surfaces in general (Mantel and Farmer, 1983). However, to counterbalance urinary salt loss and that from passive diffusion across permeable body surface areas, mainly NaCl is actively taken up from fresh water against a large gradient. While amphibians actively absorb NaCl across the skin, the gills of crustaceans and fish possess specialized cells responsible for active NaCl uptake (Larsen, 1988; Péqueux et al., 1988; Péqueux, 1995). Such cells are characterized by elaborate, highly amplified membrane surfaces, often intimately associated with an elevated number of mitochondria. An increased abundance of mitochondrial F-ATPase provides these cells with their substrate, ATP, which is sufficient to supply the ion-motive ATPases that drive active NaCl absorption. The Na^+/K^+-ATPase, which often consists of three different subunits, is an essential participant in osmoregulatory NaCl uptake (Therien and Blostein, 2000; Lucu and Towle, 2003). In most epithelia, this transmembrane protein is located in the basolateral membranes where it exchanges three intracellular Na^+ ions for two extracellular K^+ ions, generating electrochemical gradients used by secondary active transporters in both the apical and basolateral membranes. In

strong hyperosmoregulators like freshwater crustaceans, fish and amphibians, an apical V-ATPase activity is apparently required to complement that of the Na^+/K^+-ATPase in driving osmoregulatory ion uptake from the dilute medium. The V-type H^+-ATPase consists of two structural protein domains, a cytoplasmic V_1 domain and a membrane-spanning V_0 domain (Nelson, 1992). The V_1 domain makes up the catalytic sector and is composed of at least eight different subunits, while the V_0 domain contains the proton-translocating apparatus and consists of at least four different subunits. Owing to its specific capabilities of generating both electrochemical and pH gradients across the endo- and plasma membranes of eukaryotic cells, the heteromeric V-ATPase plays a role in many cellular functions (for a review, see Wieczorek et al., 1999).

A current model for NaCl uptake in freshwater crustaceans has been proposed based on data obtained using gills of the hyperosmoregulating, diadromous crab, *Eriocheir sinensis* (for reviews see Péqueux et al., 1988; Péqueux, 1995; Onken and Riestenpatt, 1998). Sodium uptake in this crab is Cl^--independent and proceeds *via* apical Na^+-channels and the basolateral Na^+/K^+-ATPase (Zeiske et al., 1992). Na^+-independent, chloride uptake may take place *via* apical Cl^-/HCO_3^- exchange and basolateral Cl^- channels, driven by the apical V-ATPase (Onken et al., 1991). Carbonic anhydrase (CA) may rapidly supply the intracellular substrates, H^+ and HCO_3^-, necessary for apical transporter function.

Most studies of NaCl absorption in hyperosmoregulating crabs concern diadromous or migratory species (for reviews, see Péqueux, 1995; Onken and Riestenpatt, 1998); information on true, continental, freshwater brachyurans is fairly scarce. In a recent study (Onken and McNamara, 2002) we established the South American freshwater crab, *Dilocarcinus pagei*, endemic to the Amazon and Paraguay/Paraná river basins, as a transport model for such hololimnetic crabs. Our data suggest that active, electrogenic NaCl uptake across the posterior gills of *D. pagei* occurs *via* mechanisms similar to those of other freshwater animals. However, in contrast to the known epithelia responsible for NaCl absorption from highly dilute media, Na^+ and Cl^- uptake in the posterior gills of *D. pagei* are effected across epithelia spatially separated within the gill lamellae, which exhibits a marked structural asymmetry. The epithelium of the proximal lamellar surface consists of thick cells, and generates a positive, Na^+-dependent, ouabain-sensitive, short-circuit current; the distal epithelium is composed of thin, pillar cell flanges, and generates a negative, Cl^--dependent, short circuit current, which is inhibited by diphenylamine-2-carboxylate (DPC) and acetazolamide (AZ).

To better characterize the mechanisms of gill ion absorption in hololimnetic crabs, in the present investigation we analyze the microanatomy, expression of mRNA and the activity of ion-motive ATPases in the anterior and posterior gills of *D. pagei*. We also provide electrophysiological data that support a role for apical V-ATPases in active, transbranchial Cl^- uptake.

Materials and methods

Crabs

Intermoult *Dilocarcinus pagei* Stimpson, measuring 4.5–5.5 cm carapace width, were collected from a temporary, floodplain pool close to the Mogi-Guaçu river (São Paulo State, Brazil). In the laboratory, the crabs were kept under a natural, light/dark photoperiod, at 20–25°C, in large tanks containing aerated tap water to a depth of approximately 10 cm, replaced two to three times per week. Aquatic plants and hollow bricks provided refuge and free access to a dry surface, respectively. The crabs were fed lettuce and/or shrimp tails three times a week.

To obtain the gills, the crabs were quickly killed by destroying the dorsal brain and the ventral ganglia using large scissors. The carapace was removed and anterior gill no. 4 and posterior gill no. 7 were excised at their bases with fine scissors, and removed with tweezers (see also Onken and McNamara, 2002). The gills were immediately prepared for light microscopic analysis and physiological experiments, or stored in RNA Later buffer (Ambion; Austin, Texas, USA) for subsequent RNA isolation.

Microscopic studies

After dissection on ice, the gills were immediately perfused *via* the afferent vessel over a 2–3 min period with 1 ml ice-cold, primary fixative containing (in mmol l^{-1}): paraformaldehyde 200, glutaraldehyde 250, and Na^+ 100, K^+ 10, Ca^{2+} 13, Mg^{2+} 2 (as chlorides), buffered in 100 mmol l^{-1} sodium cacodylate, at pH 7.5. Medial portions of selected gills consisting of approximately five lamellae each were then fixed on ice in fresh primary fixative for 1.5 h. After rinsing in buffered saline alone (3×5 min), the gill lamellae were post-fixed in 1% osmium tetroxide in buffered saline for 1 h, dehydrated in an ethanol/propylene oxide series and embedded in Araldite 502 resin. Thick (0.5 μm) sections were prepared using a Porter-Blum Sorvall MT-2B ultramicrotome and stained using a mixture of 1% methylene and Toluidine Blue in 1% aqueous borax. Digital images of sections at 200–400× magnification were taken using a Zeiss Axiophot microscope and Zeiss AxioVision 3 image acquisition software.

Molecular cloning of partial Na^+/K^+-ATPase and V-type H^+-ATPase cDNA sequences

The total RNA from anterior gill no. 4, and from posterior gill no. 7, respectively, was extracted under RNAse-free conditions using reagents supplied by Promega Corporation. After DNAse I treatment (Gibco-BRL/Invitrogen, Karlsruhe, Germany), mRNA reverse transcription was performed using oligo(dT) primers and Superscript II reverse transcriptase (Gibco-BRL/Invitrogen, Karlsruhe, Germany).

Degenerate primers, previously used successfully with other crab species for the Na^+/K^+-ATPase (α-subunit), primer pair NAK 10F/NAK 16R (Towle et al., 2001), and for the V-type H^+-ATPase (B-subunit), primer pair HATF2/HATR4 (Weihrauch et al., 2001) (see Table 1), were employed in a

Table 1. *Oligonucleotide primers used to amplify α-subunit (Na^+/K^+-ATPase) and B-subunit (V-type H^+-ATPase) cDNA from* Dilocarcinus pagei *gills*

Primer	Nucleotide sequence (5′–3′)
Na^+/K^+-ATPase	
Degenerate sense primer, NAK 10F	ATGACIGTIGCICAYATG
Degenerate antisense primer, NAK 16R	GGRTGRTCICCIGTIACCAT
V-type H^+-ATPase	
Degenerate sense primer, HATF2	GCNATGGGNGTNAAYATGGA
Degenerate antisense primer, HATR4	TGNGTDATRTCRTCGTTNGG
Specific sense primer, DiloHATF1	GTCGTCGTTGGGCATAGTAAGAAT
Specific antisense primer, DiloHATR1	ATCCAACCATCGAACGTATCATCA

D, replaces A/G/T; N and I, replace A/C/G/T; R, replaces A/G; Y, replaces C/T.

polymerase chain reaction (PCR) procedure (REDTaq, Sigma, Taufkirchen, Germany) to initially amplify the partial cDNA for both cation pumps from *D. pagei* gills.

PCR products were separated electrophoretically on 1% agarose gels, extracted from the gel slices (Qiagen, Valencia, CA, USA), and sequenced automatically using the dideoxynucleotide method (Sanger et al., 1977) at the Marine DNA Sequencing Center of Mount Desert Island Biological Laboratory, Maine, USA employing the degenerate PCR primers in the sequencing reaction. Fragment sequences were assembled using DNASTAR software and were analyzed for open reading frames employing DNASIS. A search of GenBank using the BLAST algorithm (Altschul et al., 1997) revealed close matches with sequences previously published for the Na^+/K^+-ATPase (α-subunit) and the V-type H^+-ATPase (B-subunit). The sequences obtained were then employed to design specific primers for *D. pagei* (Table 1) using Primer Premier software. Multiple alignments were performed with Multalin (Corpet, 1988) and GeneDoc software (http://www.psc.edu/biomed/genedoc/). A phylogenetic tree was generated using Drawtree (Felsenstein, 1993).

Semi-quantitative RT-PCR

The relative abundance of the Na^+/K^+-ATPase α-subunit and the V-type H^+-ATPase B-subunit in total RNA extracts was estimated by semi-quantitative RT-PCR using identical amounts (2 μg) of total RNA in each reverse transcription reaction. The PCR procedure was performed under conditions in which product formation was directly dependent on cDNA template availability. To illustrate, as shown in Fig. 1, different amounts (0.25, 0.5 and 1 μl) of template cDNA were employed in a polymerase chain reaction (primers DiloHATF1/DiloHATR1, see Table 1) using a number of cycles in which PCR product amplification was clearly in the logarithmic phase (23 cycles). Band densities were estimated under UV light by digital analysis using a Kodak Digital Science DC 120 Zoom Digital Camera and Kodak Digital Science 1D 2.0.2 software (Kodak).

ATPase activity measurements

Gills were homogenized on ice using a 1 ml glass homogenizer in ice-cold homogenization buffer, containing 10 mmol l^{-1} Hepes, 5 mmol l^{-1} EDTA and 250 mmol l^{-1} sucrose (pH 7.25). For V-ATPase activity measurements, the homogenization buffer also contained 4.5 mmol l^{-1} mercaptoethanol and 0.05% (w/v) $C_{12}E_{10}$.

ATPase activities were estimated according to the method of Onishi et al. (1976) and quantified as released inorganic phosphate. SDS activation and measurement of Na^+/K^+-ATPase activity were performed according to the method of Kosiol et al. (1988), using 10–20 μg protein in each assay. Na^+/K^+-ATPase activity was defined as the difference in SDS-activated activities obtained with or without 5 mmol l^{-1} ouabain (a Na^+/K^+ATPase inhibitor). Mitochondrial F_1F_0-ATPase activity was estimated similarly; however, inhibition by 1 mmol l^{-1} sodium azide was used to define F_1F_0-ATPase activity.

To measure V-ATPase activity, a reaction buffer containing 50 mmol l^{-1} Mops–Tris, 1 mmol l^{-1} sodium vanadate (inhibition of P-type ATPases), 1 mmol l^{-1} sodium azide (inhibition of F_1F_0-ATPase), 0.01% (w/v) $C_{12}E_{10}$, 3 mmol l^{-1} Tris–ATP and 3 mmol l^{-1} $MgCl_2$ (pH 8.0) was preincubated for 10 min at 30°C. The reaction was initiated by adding the respective gill homogenate (50–100 μg protein), and after 30 min, the amount of phosphate released was measured as above (Kosiol et al.,

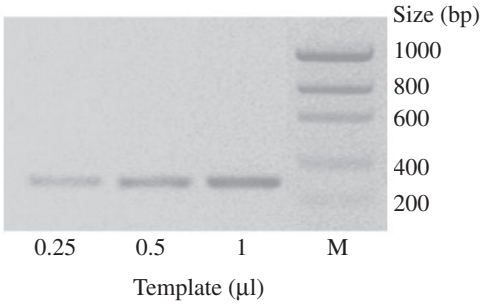

Fig. 1. Agarose gel showing template-dependent, product abundance during the logarithmic phase of PCR amplification. 2 μg total RNA, isolated from the posterior gills of *Dilocarcinus pagei*, were employed in the reverse transcription assay. Different volumes (0.25, 0.5 or 1 μl) of the resulting cDNA were used to perform 23 PCR amplification cycles. Lane M is a DNA ladder.

1988). V-ATPase activity was defined as the difference between the activities obtained with or without 1 μmol l^{-1} concanamycin (a V-ATPase inhibitor; Dröse and Altendorf, 1997).

Protein content was measured according to Bradford's method (Bradford, 1976), modified following Sedmark and Grossberg (1977), with bovine serum albumin as the standard.

Electrophysiological measurements

Gill lamellae were isolated from a medial portion of the posterior gills and mechanically split using two pairs of ultra-fine tweezers (cf. Onken et al., 1991). Distal split lamellae were mounted using a dissecting microscope in a modified Ussing chamber, such that an epithelial surface area of 0.01 cm^2 was exposed to the chamber compartments (approximately 50 μl volume) bathing the respective external and internal surfaces of the split lamella. Both chamber compartments were continuously perfused with aerated hemolymph-like saline (see Onken and McNamara, 2002) by gravity flow at a rate of approximately 2 ml min^{-1}. For voltage measurements, calomel electrodes were connected via agar bridges (3% agar in 3 mol l^{-1} KCl) to both sides of the preparation, the distance from the bridge tip to the tissue being less than 1 mm. The reference electrode was placed in the internal, hemolymph-side bath. Silver wires coated with AgCl served as electrodes to apply current for short-circuiting the transepithelial voltage (i.e. measurement of the short-circuit current, I_{sc}) through an automatic clamping device (model VCC 600; Physiologic Instruments, San Diego, CA, USA). The conductance of the preparations (G_{te}) was calculated from imposed voltage pulses (ΔV) and the resulting current deflections (ΔI). The data were recorded continuously on a chart recorder (type 3229 I/85; Linseis, Germany).

Statistical analyses

All data are given as the mean ± S.E.M. Differences between mean values were compared using Student's *t*-test, employing a significance level of P=0.05.

Results

Microanatomy

The microanatomy of the anterior and posterior gill lamellae of *Dilocarcinus pagei* differs markedly as demonstrated in sections taken transversely through a lamella from anterior gill no. 4, and through the central, osmiophilic region of a lamella from posterior gill no. 7 (Fig. 2). The epithelia underlying the cuticle on both sides of the anterior gill lamellae are symmetrical, consisting of the very thin (2–5 μm), vesiculated, apical flanges of the epithelial pillar cells, separated by an ample hemolymph space partially occupied by a discontinuous septum (Fig. 2A). However, the opposing epithelia of the posterior gill lamellae, separated by an irregular hemolymph space and traversed by occasional, slender, pillar cell perikarya, are notably structurally asymmetrical: the epithelial cells measure 3–10 μm in height on the distal side, and 18–20 μm on the proximal side (Fig. 2B). The thin, distal epithelium consists of extensive, apical flanges, well developed above the pillar cell bodies but laterally attenuated, populated by numerous, apical vesicles and invaginations. The thick, proximal epithelium is characterized by dense, columnar cells, with a large, spherical nucleus and numerous, basal invaginations with a few apical vesicles and invaginations.

mRNA expression of Na^+/K^+-ATPase and V-type H^+-ATPase

To identify expression of the Na^+/K^+-ATPase α-subunit and

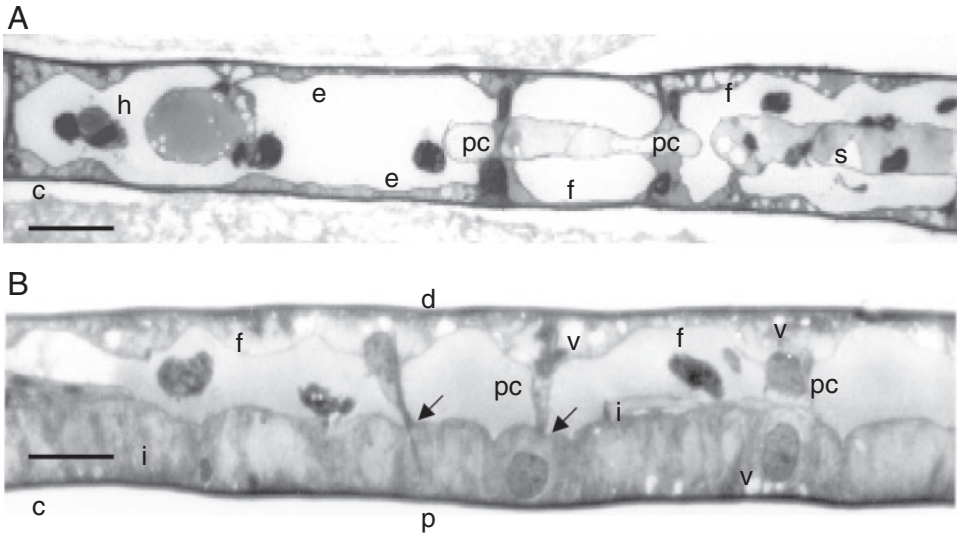

Fig. 2. Photomicrographs of transverse, 0.5 μm thick, epoxy-resin sections taken through the anterior and posterior gill lamellae of the freshwater, trichodactylid crab, *Dilocarcinus pagei*. (A) Microanatomy of a typical, medial lamella from anterior gill no. 4, showing the identical, very thin (2–5 μm) epithelia (e), symmetrically arranged on both sides of the lamella, separated by the ample hemolymph space (h), which contains a discontinuous septum (s) and hemocytes. Both epithelia consist of the very attenuated, lateral, apical flanges (f) that emerge from the pillar cell perikarya (pc) underlying the fine cuticle (c). Bar, 20 μm. (B) Architectural organization of the dense, osmiophilic, central region of a typical, medial lamella from posterior gill no. 7, revealing the highly asymmetrical nature of the distal (d) and proximal (p) epithelia underlying the thickened cuticle (c). The well-developed, distal epithelium measures 3–10 μm in thickness and consists exclusively of the extensive, apical flanges (f) of the pillar cells (pc), populated by numerous apical vesicles (v) and invaginations. The dense, proximal epithelial cells measure 18–20 μm in thickness and are characterized by large, spherical nuclei, numerous basal and apical invaginations (i), and a few apical vesicles. The lamellar septum is absent, and the distal pillar cell perikarya traverse the hemolymph space, abutting directly on the opposing, thick, proximal epithelial cells (arrows). Bar, 20 μm.

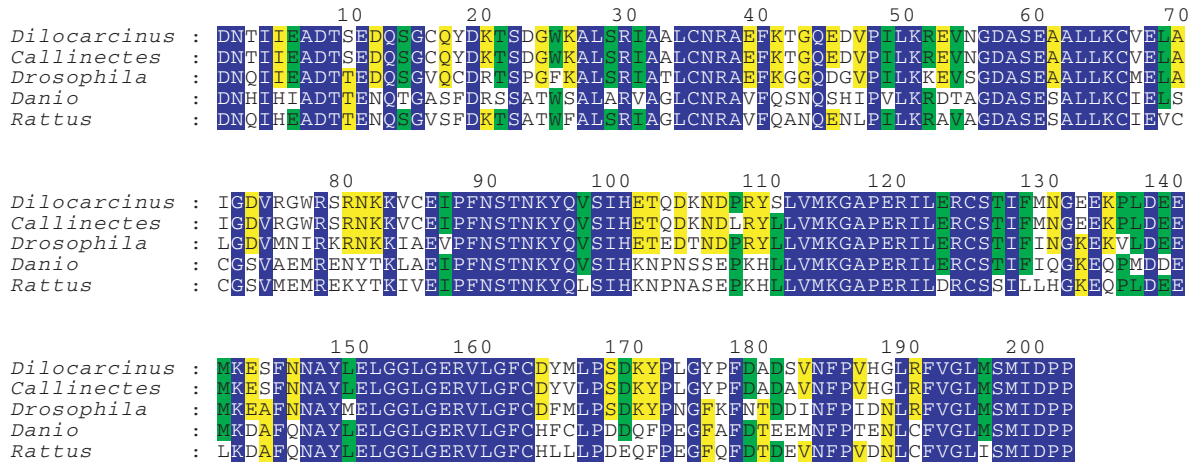

Fig. 3. Alignment of the deduced partial amino acid sequence for *Dilocarcinus pagei* Na^+/K^+-ATPase α-subunit with representative invertebrate and vertebrate sequences, including blue crab *Callinectes sapidus* (AF327439), fruit fly *Drosophila melanogaster* (AY069184), zebrafish *Danio rerio* (NM_131688) and rat *Rattus norvegicus* (M28647). Alignment was produced using Multalin (Corpet, 1988) and GeneDoc software. Blue color denotes identical amino acids (aa) in all sequences; green, identical aa in four of the five sequences; yellow, identical aa in three of the five.

V-type H^+-ATPase B-subunit in gill epithelia of the freshwater crab, *D. pagei*, we employed degenerate oligonucleotide primer pairs (NAK F10/NAK 16R for the α-subunit, and HATF2/HATR4 for the B-subunit, see Table 1), known to specifically amplify the desired target sequences in other crab species (Weihrauch et al., 2001; Towle et al., 2001). PCR amplification, employing the primer pair NAK F10/NAK 16R, resulted in a 700 bp product, which was gel-purified and sequenced. A BLAST search of GenBank clearly identified the amplified sequence as a Na^+/K^+-ATPase α-subunit fragment (GenBank accession no. AF409119). Comparison of the deduced amino acid sequence revealed a high homology with the Na^+/K^+-ATPase α-subunits of other invertebrate and vertebrate species (Fig. 3). Employing the primer combination HATF2/HATR4 resulted in a 392 bp product (GenBank accession no. AF409118). After gel purification and sequencing, a BLAST search of GenBank revealed extremely high homologies between the derived amino acid sequence for the putative H^+-ATPase B-subunit from *D. pagei* and H^+-ATPase B-subunits from other invertebrate and vertebrate species (Fig. 4). A phylogenetic analysis of the B-subunit cDNA sequences from *D. pagei*, *Carcinus maenas* (GenBank accession no. AF189779), *Callinectes sapidus* (GenBank accession no. AF189780), *Eriocheir sinensis* (GenBank accession no. AF189782), *Chasmagnathus granulata* (GenBank accession no. AF189783) and *Cancer irroratus* (GenBank accession no. AF189781) revealed the expected phylogenetic relationships among these species: *C. maenas* and *C. sapidus* in the Portunidae (0.0706 percentage divergence), *E. sinensis* and *C. granulata* in the Varunidae (Martin and Davis, 2001) (0.0161 percentage divergence), *D. pagei* in the Trichodactylidae, and *C. irroratus* in the Cancridae (Fig. 5). Both *D. pagei* and *C. irroratus* maintain large phylogenetic distances from the portunid species (0.1–0.12 and 0.11–0.13 percentage divergence, respectively) and the varunid species (1.1–1.2 and 1.4 percentage divergence, respectively).

To evaluate the importance and distribution of the Na^+/K^+-ATPase and the V-ATPase within the gills of the true freshwater crab, *D. pagei,* mRNA expression analysis and enzyme activity measurements were performed.

Semi-quantitative RT-PCR

Semi-quantitative RT-PCR clearly revealed that the mRNA for both ion pumps, the Na^+/K^+-ATPase (α-subunit) and the V-ATPase (B-subunit) are more highly expressed in the posterior than anterior gills. Compared to the PCR signal for posterior gills, amplification of both ATPases in the anterior gills required two additional PCR logarithm-phase cycles to produce equivalent or lower signals (Fig. 6).

ATPase activities

The protein content and activities of the Na^+/K^+-ATPase, the V-type H^+-ATPase and the F_1F_0-ATPase were measured in the anterior and posterior gills of *D. pagei* (Table 2). Both protein content and Na^+/K^+-ATPase activity were significantly higher in the posterior compared to anterior gills. F_1F_0-ATPase and V-type H^+-ATPase activities did not differ significantly between anterior and posterior gill homogenates.

Electrophysiological measurements

Onken and McNamara (2002) have shown that ouabain inhibits the positive, Na^+-dependent, short-circuit current (I_{sc}) across the thick, proximal, split lamellae of *D. pagei* posterior gills when mounted in an Ussing-type chamber. Here, we examined the effects of ouabain and concanamycin on the negative, Cl^-dependent I_{sc}, and on preparation conductance (G_{te}) in the thin, distal, split lamellae. While internal ouabain (2 mmol l^{-1}) had no significant effect on I_{sc}, internal concanamycin (10 μmol l^{-1}) significantly reduced I_{sc} by

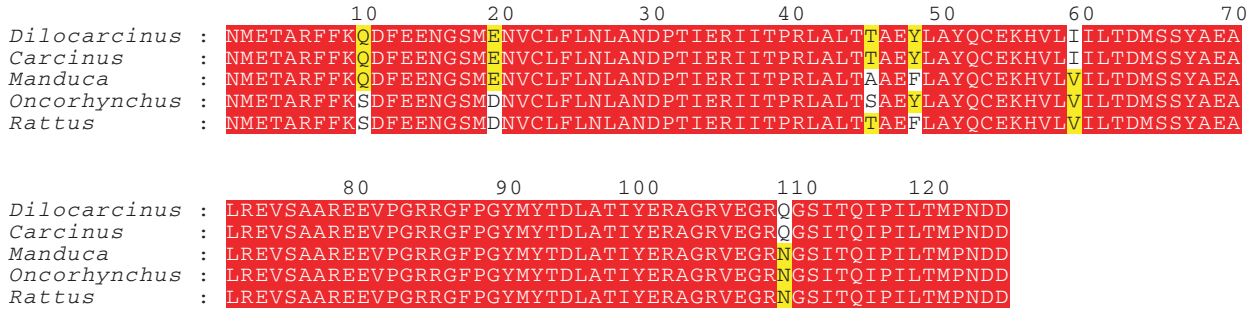

Fig. 4. Alignment of the deduced partial amino acid sequence for *Dilocarcinus pagei* V-type H^+-ATPase B-subunit with representative invertebrate and vertebrate sequences, including green shore crab *Carcinus maenas* (AF189779), tobacco hornworm *Manduca sexta* (X64354), steelhead trout *Oncorhynchus mykiss* (AAD33861) and rat *Rattus norvegicus* (NM_057213). Alignment was produced using Multalin (Corpet, 1988) and GeneDoc software. Red color denotes identical amino acids in all sequences; yellow, identical aa in three of the five.

approximately 50%, from –43±3 to –22±1 μA cm^{-2} (mean ± S.E.M.; N=3; P<0.05) without affecting transepithelial conductance (G_{te}). External concanamycin produced only a minor effect on I_{sc}. A representative experiment is shown in Fig. 7.

Discussion

Striking differences have been demonstrated between the anterior and posterior gills of hyperosmoregulating crabs that migrate between the sea and brackish or fresh waters (Péqueux et al., 1988; Taylor and Taylor, 1992; Péqueux, 1995). While the anterior gill lamellae are lined by a very thin epithelium, those of the posterior gills show structural features typical of transporting epithelia, i.e. thick cells displaying apical and basolateral membrane foldings associated with an elevated number of mitochondria. The posterior gills participate in active, electrogenic NaCl absorption as reflected in net influxes, transepithelial voltages and/or short-circuit currents, while the anterior gills do not actively absorb NaCl. The posterior gills also exhibit augmented expression and ion-motive ATPase activity compared to anterior gills. These differences constitute the basis of the paradigm that anterior gills are structurally and functionally specialized for respiratory gas exchange, while the posterior gills have become specialized in active NaCl absorption, counterbalancing passive salt loss by crabs in dilute media.

Consequent to an initial study by Onken and McNamara (2002), the present investigation provides a detailed structural and functional analysis of the gill epithelium in a true freshwater crab. In general, the known specializations of the anterior and posterior gills of diadromous crabs are also present in the hololimnetic crab, *D. pagei*. However, the gills of *D. pagei* also exhibit striking modifications to this pattern that may constitute a general feature of the trichodactylid crabs.

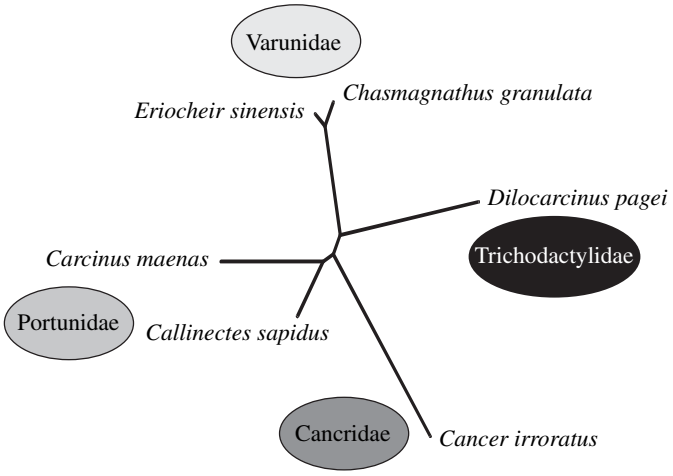

Fig. 5. Phylogenetic relationships among partial nucleotide sequences for the V-type H^+-ATPase B-subunit obtained from different brachyuran crabs. An unrooted tree was produced using Multalin (Corpet, 1988) and Drawtree (Felsenstein, 1993).

Gill microanatomy

Onken and McNamara (2002; see also Fig. 2) described a significant structural asymmetry in the posterior gill lamellae of *D. pagei*, apparently unique among crabs studied so far. While the proximal side of the lamella is lined by a thick epithelium, similar to that found symmetrically distributed on both sides of the ion transporting cell patches in the posterior lamellae of diadromous crabs (see Taylor and Taylor, 1992), the distal side has a fine epithelium consisting exclusively of thin pillar cell flanges. Thus, unlike the diadromous crabs, the distal side of the posterior gill lamellae in *D. pagei* may contribute substantially to respiratory gas exchange. Since a dense osmiophilic area, which delimits the thick epithelium, was found only in the posterior gills, analysis of the structural asymmetry lead to the premise that hololimnetic crab gills might exhibit adaptations different from those of diadromous crab gills. Thus, the present investigation directly compares the microanatomy of the anterior and posterior gill lamellae. The anterior gills of *D. pagei* are symmetrically and uniformly lined by a very attenuated epithelium (see Fig. 2A), similar to the situation in diadromous crabs. Comparison of this anterior lamellar epithelium with the thin, distal epithelium of the posterior gill lamellae shows that the latter is several times

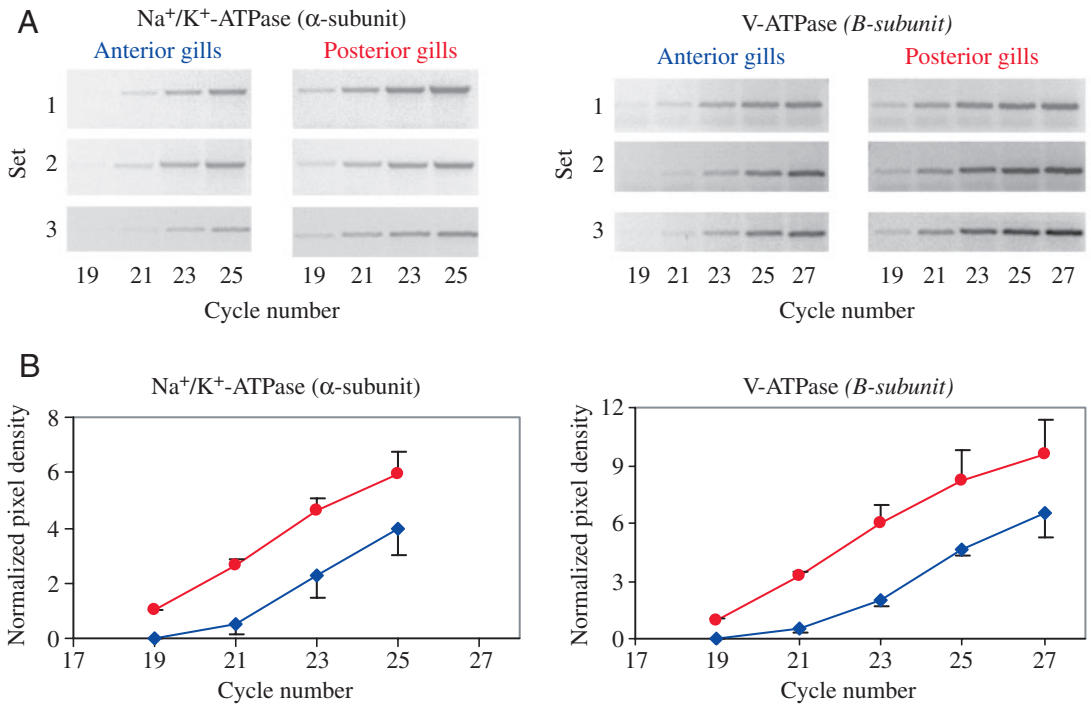

Fig. 6. Semi-quantitative reverse transcriptase/polymerase chain reaction (RT-PCR) analysis of Na^+/K^+-ATPase α-subunit and V-type H^+-ATPase B-subunit mRNA abundance in gill homogenates from *Dilocarcinus pagei*. In all experiments, PCR was performed using 1 µl cDNA, which was 5% of the cDNA reverse transcribed from 2 µg total RNA. The primer pairs NAK 10F/NAK 16R and DiloHATF1/DiloHATR1 were employed to amplify the Na^+/K^+-ATPase α-subunit and V-type H^+-ATPase B-subunit, respectively. (A) Demonstration of template-dependent quantification of Na^+/K^+-ATPase α-subunit (left panels) and V-type H^+-ATPase B-subunit (right panels) in anterior and posterior gills of *D. pagei*. (B) Graphs corresponding to data in A, showing the digitized pixel densities of the PCR products. Blue diamonds, anterior gills; red circles, posterior gills. Values are means ± S.E.M. (*N*=3).

thicker, but, exhibiting more pronounced apical membrane foldings and vesicles, reflecting a larger surface area. Thus, the present morphological findings suggest that the anterior gills of *D. pagei* share the same specialization for respiratory gas exchange as the diadromous species. On a more microanatomical, architectural level, the extraordinary difference between *D. pagei* and diadromous species is restricted exclusively to the posterior gills. The notably different thicknesses of the proximal and distal epithelia of the posterior gill lamellae derive from two special features. First, the posterior lamellae of diadromous crabs have pillar cells on both sides of the lamella, but in *D. pagei* this cell type is restricted to the distal side. Second, the pillar cells of *D. pagei* exhibit very broad, laterally attenuated, apical flanges, a feature not seen in similar cells from diadromous species. Interestingly, however, a similar structural arrangement is encountered in the gills of freshwater, palaemonid shrimps (Freire and McNamara, 1995; McNamara and Lima, 1997), also very efficient hyperosmoregulators (Freire et al., 2003).

Ion-motive ATPases

Transepithelial ion transport derives from the activity of members of three ion-motive ATPase families. While mitochondrial F-ATPases generate ATP, functioning as ATP synthetases under physiological conditions, P-ATPases and V-ATPases use ATP to generate and maintain transmembrane ionic gradients subsequently used as an energy source by passive transporters. P-ATPases and V-type H^+-pumps thus constitute the motors of transmembrane and transepithelial transport.

The analysis of mRNA expression of the Na^+/K^+-ATPase α-

Table 2. *Protein content and mean ATPase activities of Na^+/K^+-ATPase, F_1F_0-ATPase and V-ATPase in homogenates of anterior and posterior gills from the hololimnetic freshwater crab* Dilocarcinus pagei

Gill	Na^+/K^+-ATPase	F_1F_0-ATPase	Protein	V-type ATPase	Protein
Anterior	5.5±1.9	8.2±2.5	46±7.2	0.27±0.05	58±5.9
Posterior	19.3±1.6*	9.2±0.9	68±5.3*	0.39±0.10	72±8.6*

ATPase activities are given in µmol min^{-1} g^{-1} FW, and protein content in mg protein g^{-1} FW. Values are mean ± S.E.M; *N*=6–8; *$P \leqslant 0.05$ compared to anterior gills.

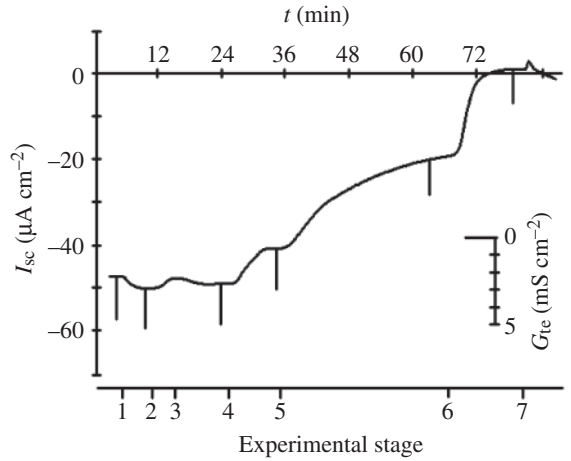

Fig. 7. Representative time-course of the short-circuit current (I_{sc}) across a distal split lamella from a posterior gill of *Dilocarcinus pagei*. The vertical current deflections are the responses to 4 mV voltage pulses, and are directly proportional to the transepithelial conductance (G_{te}, see separate scale bar). Experimental stages: 1, addition of internal ouabain (2 mol l^{-1}); 2, ouabain washout; 3, symmetrical addition of DMSO (0.1%); 4, external concanamycin (10 μmol l^{-1}); 5, internal concanamycin (10 μmol l^{-1}); 6, washout of DMSO and concanamycin, and internal addition of NaCN (5 mmol l^{-1}); 7, NaCN washout.

subunit and the V-ATPase B-subunit clearly indicates that both cation pumps are expressed in the gill tissue of the freshwater crab, *D. pagei*. As shown in Figs 3 and 4, both the α-subunit of the Na^+/K^+-ATPase and the B-subunit of the V-ATPase are highly conserved across the animal kingdom. The deduced, partial amino acid sequence of the Na^+/K^+-ATPase α-subunit from *D. pagei* (202 amino acids) was 95–99% homologous with the α-subunit sequences of other crab species published in GenBank. An even higher homology (99–100% identities) with other crab species was found on comparing the partial amino acid sequences of the B-subunit (V-ATPase, 124 amino acids). The cDNA sequence of this highly conserved region of the B-subunit was therefore used for a phylogenetic analysis among crab species. The result, shown in Fig. 5, confirms the previous classification and grouping based on morphological criteria

mRNA expression and enzyme activity measurements of the Na^+/K^+-ATPase in *D. pagei* showed significantly higher levels in the posterior compared to anterior gills (see Fig. 6), consistent with molecular biological and physiological studies on other crab species (Siebers et al., 1982; Onken and Putzenlechner, 1995; Towle and Weihrauch, 2001; Lucu and Towle, 2003), which have designated the posterior gill epithelium, with its high abundance and Na^+/K^+-ATPase activity, as the principal site of osmoregulatory ion transport. Greater expression of V-ATPase mRNA was also detected in posterior compared to anterior gills; however, V-ATPase activities did not differ significantly between anterior and posterior gills. This contrasts with findings from freshwater-adapted Chinese crabs, *Eriocheir sinensis*, where enzyme activity (Onken and Putzenlechner, 1995) and mRNA expression (Weihrauch et al., 2001) are significantly higher in posterior compared to anterior gills.

In the present study on *D. pagei*, we employed the same assay used by Onken and Putzenlechner (1995) to measure ATPase activities in *E. sinensis*. A comparison of the data shows that the posterior gills of *E. sinensis* exhibits markedly higher F-, V- and Na^+/K^+-ATPase activities than those of *D. pagei*. This difference may reflect a smaller passive salt loss in *D. pagei*, and thus, lower, compensatory active NaCl absorption. In particular, low passive salt losses have been reported in hololimnetic crabs (Shaw, 1959; Harris, 1975; Greenaway, 1981; Morris and Van Aardt, 1998). While the activities of all three ATPases are markedly reduced in the anterior gills of *E. sinensis*, in *D. pagei* the anterior and posterior gills exhibit similar V- and F-ATPase activities, which suggests that the anterior gills of *D. pagei* may generate ATP for an as-yet-unknown V-ATPase-driven process. One possibility is branchial ammonium excretion. In the euryhaline crab *Carcinus maenas*, where V-ATPases seem not to be involved in gill osmoregulatory NaCl uptake, V-ATPase mRNA levels are higher in the anterior gills (Weihrauch et al., 2001), and higher active ammonia transport rates have been found in the anterior compared to posterior gills (Weihrauch et al., 1998). Furthermore, V-ATPases are directly involved in transbranchial ammonia transport in *C. maenas* (Weihrauch et al., 2002). Whether V-ATPase activity in the anterior gills of *D. pagei* is also related to increased branchial ammonia excretion remains to be evaluated in further studies.

Transbranchial NaCl absorption

Onken and McNamara (2002) demonstrated that the opposing sides of the posterior gill lamellae in *D. pagei* generated short-circuit currents (I_{sc}) of opposite polarity. With perfusion of identical salines on both sides, the thick, proximal epithelium generated a positive I_{sc} dependent on Na^+ ions, and inhibited by hemolymph-side ouabain. The thin, distal epithelium generated a negative I_{sc}, dependent on Cl^- ions, and inhibited by hemolymph-side, Cl^- channel and carbonic anhydrase blockers. These authors proposed that an apparently independent absorption of Na^+ and Cl^- is reflected in such currents and takes place across the different sides of the lamellae: Na^+/K^+-ATPase-driven Na^+ absorption across the proximal epithelium, and V-ATPase-driven Cl^- absorption across the distal epithelium. In the present study, we used concanamycin to evaluate the role of V-ATPase in generating the negative, Cl^--dependent I_{sc}. While addition of the Na^+/K^+ATPase inhibitor ouabain (Skou and Hilberg, 1969) to the hemolymph-side had no effect on the negative I_{sc}, the V-ATPase inhibitor concanamycin (Huss et al., 2002) significantly reduced this current (Fig. 7), a result that indicates that the negative current is indeed independent of a functioning Na^+/K^+-ATPase, and that Cl^- transport is apparently driven by the V-ATPase. In the NaCl-absorbing epithelia of freshwater animals, V-ATPases are usually localized in the apical membrane where they drive Na^+ and/or Cl^- absorption (Kirschner, 2004). However, the external application of concanamycin to the distal side of the posterior gill lamella in *D. pagei* had only a minor effect on the negative I_{sc} (Fig. 7). A

basolateral localization of the V-ATPase could not account for this negative I_{sc} and its inhibition by concanamycin. Thus, we propose that internally perfused concanamycin exerts its effect only after diffusing to the apical membrane, and that externally applied concanamycin either does not, or barely reaches its site of action, owing to the thick cuticle covering the apical membrane. Clearly, further studies are necessary to establish the location of the V-ATPase in this epithelium.

This study was supported by research grants from the Deutscher Akademischer Austauschdienst (DAAD/GTZ) Germany to H.O. and J.C.M., and by the National Science Foundation (IBN-9807539) to D.W. and D.W.T. H.O. acknowledges research support through a Visiting Professorship from CAPES (Brazil) / DAAD (Germany), and J.C.M. a research scholarship from the Conselho Nacional de Desenvolvimento Científico e Tecnológico (CNPq #303282/84-3).

References

Altschul, S. F., Madden, T. L., Schaffer, A. A., Zhang, J., Zhang, Z., Miller, W. and Lipman, D. J. (1997). Gapped BLAST and PSI-BLAST: a new generation of protein database search programs. *Nucleic Acids Res.* **25**, 3389-3402.

Bradford, M. M. (1976). A rapid and sensitive method for the quantitation of microgram quantities of protein utilizing the principle of protein-dye binding. *Anal. Biochem.* **72**, 248-254.

Corpet, F. (1988). Multiple sequence alignment with hierarchical clustering. *Nucleic Acids Res.* **16**, 10881-10890.

Dröse, S. and Altendorf, K. (1997). Bafilomycins and concanamycins as inhibitors of V-ATPases and P-ATPases. *J. Exp. Biol.* **200**, 1-8.

Felsenstein, J. (1993). PHYLIP (Phylogeny Inference Package) version 3.5c. Department of Genetics, University of Washington, Seattle.

Freire, C. A. and McNamara, J. C. (1995). Fine structure of the gills of the fresh-water shrimp *Macrobrachium olfersii* (Decapoda): effect of acclimation to high salinity and evidence for involvement of the lamellar septum in ion uptake. *J. Crust. Biol.* **15**, 103-116.

Freire, C. A., Cavassin, F., Rodrigues, E. N., Torres, A. H., Jr and McNamara, J. C. (2003). Adaptive patterns of osmotic and ionic regulation, and the invasion of freshwater by the palaemonid shrimps. *Comp. Biochem. Physiol.* **136A**, 771-778.

Greenaway, P. (1981). Sodium regulation in the freshwater/land crab *Holthuisana transversa*. *J. Comp. Physiol.* **142B**, 451-456.

Harris, R. R. (1975). Urine production rate and urinary sodium loss in the freshwater crab *Potamon edulis*. *J. Comp. Physiol.* **96**, 143-153.

Huss, M., Ingenhorst, G., Konig, S., Gassel, M., Drose, S., Zeeck, A., Altendorf, K. and Wieczorek, H. (2002). Concanamycin A, the specific inhibitor of V-ATPases, binds to the V(o) subunit c. *J. Biol. Chem.* **277**, 40544-40548.

Kirschner, L. B. (2004). The mechanism of sodium chloride uptake in hyperregulating aquatic animals. *J. Exp. Biol.* **207**, 1439-1452.

Kosiol, B., Bigalke, T. and Graszynski, K. (1988). Purification and characterization of gill (Na^+, K^+)-ATPase in the freshwater crayfish *Orconectes limosus* Rafinesque. *Comp. Biochem. Physiol.* **89**, 171-177.

Larsen, E. H. (1988). NaCl transport in amphibian skin. In *Advances in Comparative and Environmental Physiology*, vol. 1 (ed. R. Greger), pp. 189-248. Berlin: Springer.

Lucu, Č. and Towle, D. W. (2003). Na^++K^+-ATPase in gills of aquatic Crustacea. *Comp. Biochem. Physiol.* **135A**, 195-214.

Mantel, L. H. and Farmer, L. L. (1983). Osmotic and ionic regulation. In *The Biology of Crustacea*, vol. 5, *Internal Anatomy and Physiological Regulation* (ed. L. H. Mantel), pp. 53-161. New York: Academic Press.

Martin, J. W. and Davis, G. E. (2001). An updated classification of the Recent Crustacea. *Natural History Museum of Los Angeles County, Science Series* **39**, 1-124.

McNamara, J. C. and Lima, A. G. (1997). The route of ion and water movements across the gill epithelium of the freshwater shrimp *Macrobrachium olfersii* (Decapoda, Palaemonidae): evidence from ultrastructural changes induced by acclimation to saline media. *Biol. Bull Woods Hole* **192**, 321-331.

Morris, S. and van Aardt, W. J. (1998). Salt and water relations, and nitrogen excretion, in the amphibious freshwater crab *Potamonautes warreni* in water and in air. *J. Exp. Biol.* **201**, 883-893.

Nelson, N. (1992). The vacuolar H(+)-ATPase – one of the most fundamental ion pumps in nature. *J. Exp. Biol.* **172**, 19-27.

Onishi, T., Gall, R. S. and Mayer, M. L. (1976). An improved assay of inorganic phosphate in the presence of extralabile phosphate compounds: application to the ATPase assay in presence of phosphocreatine. *Anal. Biochem.* **69**, 261-267.

Onken, H. and McNamara, J. C. (2002). Hyperosmoregulation in the red freshwater crab *Dilocarcinus pagei* (Brachyura, Trichodactylidae): structural and functional asymmetries of the posterior gills. *J. Exp. Biol.* **205**, 167-175.

Onken, H. and Putzenlechner, M. (1995). A V-ATPase drives active, electrogenic and Na^+-independent Cl^- absorption across the gills of *Eriocheir sinensis*. *J. Exp. Biol.* **198**, 767-774.

Onken, H. and Riestenpatt, S. (1998). NaCl absorption across split gill lamellae of hyperregulating crabs: Transport mechanisms and their regulation. *Comp. Biochem. Physiol.* **119A**, 883-893.

Onken, H., Graszynski, K. and Zeiske, W. (1991). Na^+-independent electrogenic Cl^- uptake across the posterior gills of the Chinese crab (*Eriocheir sinensis*): Voltage-clamp and microelectrode studies. *J. Comp. Physiol.* **161B**, 293-301.

Péqueux, A. (1995). Osmotic regulation in crustaceans. *J. Crust. Biol.* **15**, 1-60.

Péqueux, A., Gilles, R. and Marshall, W. S. (1988). NaCl transport in gills and related structures. In *Advances in Comparative and Environmental Physiology*, vol. 1 (ed. R. Greger), pp. 1-73. Berlin, Heidelberg: Springer.

Sanger, F., Nicklen, S. and Coulson, A. R. (1977). DNA sequencing with chain-terminating inhibitors. *Proc. Natl. Acad. Sci. USA* **74**, 5463-5467.

Sedmark, J. J. and Grossberg, S. E. (1977). A rapid, sensitive and versatile assay for protein using Coomassie Brillant Blue G250. *Anal. Biochem.* **79**, 544-552.

Shaw, J. (1959). Salt and water balance in the East African freshwater crab, *Potamon niloticus* (M. Edw.). *J. Exp. Biol.* **36**, 157-179.

Siebers, D., Leweck, K., Markus, H. and Winkler, A. (1982). Sodium regulation in the shore crab *Carcinus maenas* as related to ambient salinity. *Mar. Biol.* **17**, 291-303.

Skou, J. C. and Hilberg, C. (1969). The effect of cations, g-strophanthin and oligomycin on the labeling from [32P] ATP of the (Na^+ + K^+)-activated enzyme system and the effect of cations and g-strophanthin on the labeling from [32P] ITP and 32Pi. *Biochim. Biophys. Acta* **185**, 198-219.

Taylor, H. H. and Taylor, E. W. (1992). Gills and lungs: the exchange of gases and ions. In *Microscopic Anatomy of Invertebrates, Vol. 10, Decapod Crustacea* (ed. F. W. Harrison), pp. 203-293. New York: Wiley-Liss Inc.

Therien, A. G. and Blostein, R. (2000). Mechanisms of sodium pump regulation. *Am. J. Physiol. Cell Physiol.* **279**, C541-C566.

Towle, D. and Weihrauch, D. (2001). Osmoregulation by gills of euryhaline crabs: molecular analysis of transporters. *Am. Zool.* **41**, 770-780.

Towle, D. W., Paulsen, R. S., Weihrauch, D., Kordylewski, M., Salvador, C., Lignot, J. H. and Spanings-Pierrot, C. (2001). Na^++K^+-ATPase in gills of the blue crab *Callinectes sapidus*: cDNA sequencing and salinity-related expression of alpha-subunit mRNA and protein. *J. Exp. Biol.* **204**, 4005-4012.

Weihrauch, D., Becker, W., Postel, U., Riestenpatt, S. and Siebers, D. (1998). Active excretion of ammonia across the gills of the shore crab *Carcinus maenas* and its relation to osmoregulatory ion uptake. *J. Comp. Physiol.* **168B**, 364-376.

Weihrauch, D., Ziegler, A., Siebers, D. and Towle, D. W. (2001). Molecular characterization of V-type H^+-ATPase (B-subunit) in gills of euryhaline crabs and its physiological role in osmoregulatory ion uptake. *J. Exp. Biol.* **204**, 25-37.

Weihrauch, D., Ziegler, A., Siebers, D. and Towle, D. W. (2002). Active ammonia excretion across the gills of the green shore crab *Carcinus maenas*: participation of Na^+/K^+-ATPase, V-type H^+-ATPase and functional microtubules. *J. Exp. Biol.* **205**, 2765-2775.

Wieczorek, H., Brown, D., Grinstein, S., Ehrenfeld, J. and Harvey, W. R. (1999). Animal plasma membrane energization by proton-motive V-ATPases. *BioEssays* **21**, 637-648.

Zeiske, W., Onken, H., Schwarz, H. J. and Graszynski, K. (1992). Invertebrate epithelial Na^+ channels: amiloride-induced current-noise in crab gill. *Biochim. Biophys. Acta* **1105**, 245-252.